Stability of the U(1) spin liquid with a spinon Fermi surface in 2+1 dimensions

Sung-Sik Lee
Department of Physics & Astronomy, McMaster University, Hamilton, Ontario, Canada L8S 4M1
(Received 12 May 2008; revised manuscript received 15 July 2008; published 25 August 2008)

We study the stability of the 2+1 dimensional U(1) spin liquid state against proliferation of instantons in the presence of a spinon Fermi surface. By mapping the spinon Fermi surface into an infinite set of 1+1 dimensional chiral fermions, it is argued that an instanton has an infinite scaling dimension for any nonzero number of spinon flavors. Therefore, the spin liquid phase is stable against instantons and the noncompact U(1) gauge theory is a good low-energy description.

DOI: 10.1103/PhysRevB.78.085129 PACS number(s): 71.27.+a, 71.10.Hf, 75.10.Jm, 75.45.+j

I. INTRODUCTION

Fractionalized phase is an unconventional phase of correlated many-body systems where low-energy excitations carry fractional quantum numbers of microscopic degrees of freedom. In 1+1D, a spin charge separation, which is an example of fractionalization, can naturally occur due to the low dimensionality.[1] In 2+1D, fractional quantum Hall states support excitations, which have fractional electric charges.[2] Finding a fractionalized phase in time-reversal symmetric 2+1D systems is an outstanding problem in condensed-matter physics.[3,4]

In fractionalized phases, there exist nonlocal correlations, which are not captured by the conventional symmetry-breaking picture.[5] Those correlations are associated with a condensation of stringy objects in space[6] or membranes in space time.[7] It turned out that the most natural framework to describe those correlations is gauge theory, where the gauge field describes transverse fluctuations of condensed strings or membranes.

Spin liquid is a fractionalized state where an elementary excitation is spinon, which carries spin 1/2 but has no charge.[3] Among a variety of possible spin liquid states,[5] the state that has fermionic spinons and an emergent U(1) gauge field has been proposed for many 2+1D strongly correlated electron systems including high-temperature superconductors, frustrated magnets, and heavy fermion systems. Although high-T_c superconductors have the conventional superconducting ground state, the normal state shows non-Fermi liquid behaviors, which are possibly due to a proximity to a spin liquid state.[4,8] Frustrated magnets are simpler systems than the high-T_c cuprates, in that there is no low-energy charge mode. At the moment, there are promising candidate materials[9,10] for which the U(1) spin liquid states with fermionic spinons have been proposed.[11–13] Related fractionalized phases have been studied in heavy fermion systems near magnetic quantum critical points[14] and frustrated Bose systems.[15] In the U(1) spin liquid states, fermionic spinons have either nodal points or Fermi surfaces. The gapless spinons are strongly coupled with the U(1) gauge field at low energies and there is no well defined quasiparticle.[16–21]

Because of underlying lattice structures, the U(1) gauge field is compact, which allows for a topological defect called instanton (or monopole). Instanton, as a localized object in space time, describes an event where the flux of the gauge field changes by 2π. Understanding dynamics of instantons is crucial because the fractionalized state is stable only if instantons are suppressed in the long-distance limit. It has been known that if there is no gapless spinon, instantons always proliferate, resulting in confinement. In this case, spin liquid states are not stable and spinons are permanently confined.[22] In the presence of gapless spinons, it is possible that the gauge field is screened and instanton becomes irrelevant in the low-energy limit. If this happens, fractionalized phase is stable and spinons arise as low-energy excitations.

If there are a large number of gapless spinons, which have the relativistic dispersion near nodal points, it has been shown that instanton is irrelevant at low energies and the fractionalized phase is stable.[23] However, it is largely unknown whether the spin liquid phase is stable in the physical cases where the number of spinon flavors is relatively small. In the presence of spinon Fermi surface, it has been speculated that the abundance of low-energy spinon modes may stabilize the fractionalized phase more easily. However, dynamics of instantons in the presence of nonrelativistic spinons has not been well understood. There have been several random-phase approximation (RPA) studies[24–29] but currently there exists no nonperturbative analysis on the fate of instantons in the presence of spinon Fermi surface. Particularly, a lack of the conformal symmetry makes it hard to treat the problem in a nonperturbative way, which is required because instanton itself is a nonperturbative phenomenon.

In this paper, we provide a nonperturbative argument, which supports the idea that the U(1) spin liquid state with spinon Fermi surface is indeed stable against proliferation of instantons for any nonzero N, where N is the number of spinon flavors. The paper consists of three main parts. In the first part (Sec. III), we ignore fluctuations of the noncompact component of the gauge field, and we calculate the scaling dimension of instanton at the fixed point described by free spinons. To do this, in Sec. II, we formulate low-energy modes near the Fermi surface in terms of an infinite number of 1+1D chiral fermions. Since an instanton is a localized source of 2π flux in space time, the fermions—which move in 1+1 dimensional subspaces—have to enclose the half of the solid angle around the instanton and acquire phase π when they are transported around the instanton at a sufficiently large distance. This is illustrated in Fig. 2. Therefore, an instanton operator corresponds to a twist operator of the 1+1D chiral fermions. The scaling dimension of an instanton is infinite because there are infinitely many 1+1D fermions parametrized by the direction of their velocities (or angular momentum) and each fermion contributes a finite scaling dimension to the total scaling dimension of the instanton operator. In the second part (Sec. IV), the fluctuations of the noncompact gauge field are considered together with instantons. To control the gauge fluctuations, we consider a large N limit. In this case, vertex corrections are negligible and we can obtain a definite scaling transformation under which the low-energy theory remains invariant. The key difference from the previous studies[19,21] is that in the present approach all points on the Fermi surface are treated on the equal footing rather than focusing on a local patch in the momentum space. This enables us to define the scaling dimension of the instanton operator, taking into account the whole Fermi surface. With the fluctuating noncompact gauge field, fermion modes—which have different Fermi velocities—are no longer decoupled, and we cannot simply sum the scaling dimensions of different modes as we did in the noninteracting case. However, in the low-energy limit, only small-angle scatterings are important because momenta of the gauge field are scaled down while the circumference of the Fermi surface is unchanged under the scale transformation. This implies that two fermion fields on different points on the Fermi surface are essentially decoupled at low energies. Therefore, there are still infinitely many independent 1+1D fermion modes, which contribute to the scaling dimension of instanton at low energies. By using this property, we can argue that the scaling dimension of an instanton is infinite also at the interacting fixed point. Finally, in Sec. V, we consider the case with a small N of the order of 1, which is directly pertinent to the U(1) spin liquid state with two flavors (spin up and down) of spinons[11,12] proposed for $\kappa-(\mathrm{BEDT-TTF})_2\mathrm{Cu}_2(\mathrm{CN})_3$.[9] With a small N, the Fermi surface is strongly coupled with the fluctuating gauge field and vertex corrections cannot be ignored. This makes it difficult to find an explicit form of a scaling transformation for the strongly interacting fixed point. However, one can see that the essential properties, which make the scaling dimension of instanton infinite, does not depend on the specific form of a scaling transformation. Actually, the existence of an extended Fermi surface and the fact that only small-angle scatterings are important at low energies are enough to argue that the scaling dimension of instanton remains to be infinite and instantons are irrelevant at a strongly interacting fixed point for any nonzero N.

II. ANGULAR REPRESENTATION OF FERMI SURFACE

We start by considering N flavors of fermions coupled with a compact U(1) gauge field in 2+1D,

$$S = \int d^3x \left[\Psi_j^*(\partial_0 - ia_0 - \mu_F)\Psi_j + \frac{1}{2m}\Psi_j^*(-i\nabla - \mathbf{a})^2\Psi_j + \frac{1}{4g^2}f_{\mu\nu}f_{\mu\nu}\right]. \tag{1}$$

Here Ψ_j is the fermion field with N flavors, $j=1,2,..,N$, and $a_\mu=(a_0,\mathbf{a})$ is the U(1) gauge field with $\mu=0,1,2$. μ_F is the chemical potential, g is the gauge coupling, and $f_{\mu\nu}$ is the field strength tensor. Summation over the repeated flavor index j is implied. In the energy-momentum space, the action becomes

$$\begin{aligned} S = &\int d^3p\left[(ip_0+\epsilon_{\mathbf{p}})\Psi_j^*(p)\Psi_j(p) + \frac{1}{2g^2}(p^2\delta_{\mu\nu} - p_\mu p_\nu)a_\mu^*(p)a_\nu(p)\right] + \int \frac{d^3p d^3l}{(2\pi)^{3/2}}\left[-ia_0(l) - \frac{\mathbf{p}\cdot\mathbf{a}(l)}{m}\right]\Psi_j^*\left(p+\frac{l}{2}\right)\Psi_j\left(p-\frac{l}{2}\right) \\ &+ \int \frac{d^3p_1d^3p_2d^3l}{(2\pi)^3}\frac{1}{2m}\mathbf{a}^*(p_2-l)\cdot\mathbf{a}(p_2)\Psi_j^*(p_1+l)\Psi_j(p_1). \end{aligned} \tag{2}$$

Here p and l denote energy-momentum vectors and $\epsilon_{\mathbf{p}}=\frac{|\mathbf{P}|^2}{2m}-\mu_F$. Integrating out high-energy fermion modes outside a momentum shell with a width Λ near the Fermi surface, we obtain the low-energy effective action $S=S_0+S_1$, where

$$S_0 = \int d\omega dk d\theta\,(i\omega+k)\psi_j^*(\omega,k,\theta)\psi_j(\omega,k,\theta) + \int d^3p\left[\frac{1}{2g^2}(p^2\delta_{\mu\nu}-p_\mu p_\nu)a_\mu^*(p)a_\nu(p) + K\mathbf{a}^*(p)\cdot\mathbf{a}(p)\right],$$

$$S_1 = -\frac{i}{(2\pi)^{3/2}}\int d\omega dk d\theta d\nu dq_l dq_t\,[a_0(\nu,q_l,q_t;\theta) - ia_\theta(\nu,q_l,q_t;\theta)]\psi_j^*\left(\omega+\frac{\nu}{2},k+\frac{q_l}{2},\theta+\frac{q_t}{2k_F}\right) \times\psi_j\left(\omega-\frac{\nu}{2},k-\frac{q_l}{2},\theta-\frac{q_t}{2k_F}\right). \tag{3}$$

Here, the Fermi velocity has been set to one. Fermion momentum is represented in the polar coordinate,[30] where $k \equiv |\mathbf{k}|-k_F$ is the deviation of momentum from the Fermi surface in the radial direction and θ is the angular coordinate as is shown in Fig. 1(a). We use the approximation, $\int d\mathbf{k} = \int d|\mathbf{k}||\mathbf{k}|\int d\theta \approx k_F\int dk\int d\theta$, and redefine the fermion field as $\psi_j(\omega,k,\theta)\equiv k_F^{1/2}\Psi_j[\omega,k_1=(k_F+k)\cos\theta,k_2=(k_F+k)\sin\theta]$. $K\sim Nk_F$ is the diamagnetic term. $a_\theta=\hat{k}_\theta\cdot\mathbf{a}$ is the spatial gauge field parallel to the fermion momentum along $\hat{k}_\theta=(\cos\theta,\sin\theta)$. $q_l=\hat{k}_\theta\cdot\mathbf{q}$ and $q_t=(\hat{k}_\theta\times\mathbf{q})_z$ are the momentum components of the gauge field, which are parallel and perpendicular to $\hat{k}_\theta$, respectively. Note that $a_0(\nu,q_l,q_t;\theta)$ and $a_\theta(\nu,q_l,q_t;\theta)$ in the second line of Eq. (3) implicitly depend on θ because q_l and q_t are measured in reference to $\hat{k}_\theta$ as shown in Fig. 1(b). Λ is the momentum cutoff of the fermions near the Fermi surface and $\tilde{\Lambda}$ is the cutoff of the gauge field. For $\Lambda \ll k_F$, we can ignore the quadratic term $k^2/2m$, which is irrelevant at low energies.

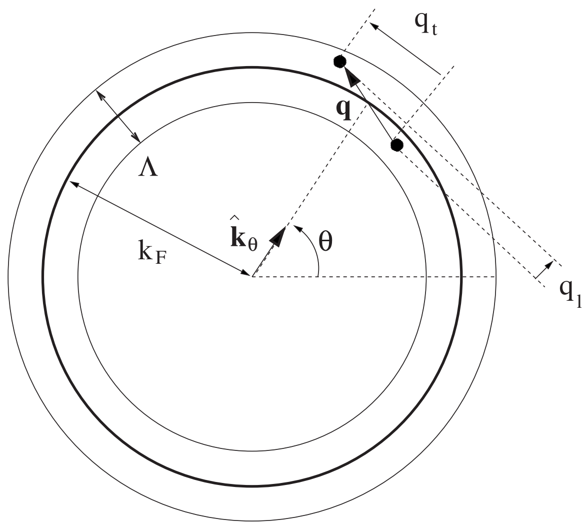

(a)

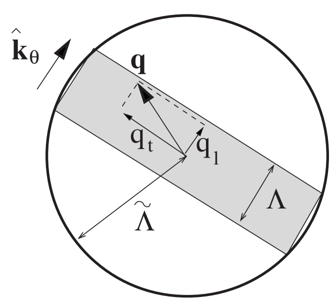

(b)

FIG. 1. Low-energy modes in the momentum space (a) for the fermions and (b) for the gauge field. Λ and $\tilde{\Lambda}$ are the cut-off momenta for the fermions and the gauge field, respectively. In (a), the bold circle represents the Fermi surface and the arrow connecting the two filled circles represents a momentum transfer from the gauge field. The shaded strip in (b) represents the points of momenta, which are included in the background gauge field felt by the 1+1D chiral fermions with angle θ, as will be discussed in Sec. III.

III. FREE FERMIONS

The gauge field can be decomposed into the singular part, which includes instanton configurations, and the nonsingular part, which describes fluctuations of the noncompact component. First, we ignore the noncompact gauge field and examine the effect of instantons on the free fermions. For this, we consider a background gauge field a_μ^s generated by an instanton located at $\tau=0$ and $\mathbf{x}=0$ in space and in time. For the singular part of the gauge field, we use the temporal gauge where $a_0^s=0$.

If the Fermi surface has the rotational symmetry, the field strength for single instanton centered at the origin has the rotational symmetry too. This enables us to choose $a_\theta^s(\nu,q_l,q_t;\theta)$ to be independent of θ. Because of the rotational symmetry, it is convenient to introduce 1+1D chiral Fermi fields, which have good angular momentum quantum number,

$$\psi_{jn}(\tau,x) = \frac{1}{(2\pi)^{3/2}}\int d\omega dk d\theta\ e^{i(\omega\tau+kx+n\theta)}\psi_j(\omega,k,\theta). \quad (4)$$

In the 1+1D real space, the action for the chiral fermions becomes

$$S=\sum_n \int d\tau dx\ \psi_{jn}^*(\tau,x)\{\partial_\tau - i[\partial_x - ia_\theta^s(\tau,x,x_t = n/k_F)]\}\psi_{jn}(\tau,x), \quad (5)$$

where the 1+1D gauge field "felt" by the chiral fermions is given by

$$a_\theta^s(\tau,x,x_t) = \frac{1}{(2\pi)^{3/2}}\int_{-\infty}^{\infty} d\omega \int_{-\Lambda/2}^{\Lambda/2} dq_l \times \int_{-\tilde{\Lambda}}^{\tilde{\Lambda}} dq_t\ e^{i(\omega\tau+q_l x+q_t x_t)} a_\theta^s(\omega,q_l,q_t;\theta). \quad (6)$$

Here x and x_t represent the displacements from the instanton in the directions parallel and perpendicular to $\hat{k}_\theta$ for some θ, respectively. Because of the rotational symmetry, $a_\theta(\tau,x,x_t)$ is independent of θ and the choice of θ does not matter. The action in Eq. (5) describes an infinite set of 1+1D chiral fermions coupled to the background gauge field, $a_\theta^s(\tau,x,x_t = n/k_F)$. The chiral fermion with angular momentum n "sees" the 2+1D gauge field projected onto a plane, which is perpendicular to the x_1-x_2 plane and shifted by n/k_F away from the origin as shown in Fig. 2(a). The range of the momentum integration in Eq. (6) is restricted to be within the strip with the width Λ, as shown in Fig. 1(b), and $a_\theta^s(\tau,x,x_t)$ represents the slowly varying configurations of the gauge field in space and in time. Nevertheless, the components with large momenta become unimportant in the long-distance limit, and $a_\theta^s(\tau,x,x_t)$ accurately describes the true configuration of instanton far away from the center. For an instanton whose field strength is isotropic in space and in time, the gauge field is given by

$$a_0 = 0,$$

$$a_1 = \frac{x_2}{2r(r-\tau)},$$

$$a_2 = -\frac{x_1}{2r(r-\tau)}, \quad (7)$$

with $r=\sqrt{\tau^2+x_1^2+x_2^2}$. In this gauge, there is a Dirac string stretched along the positive τ axis. The presence of the Dirac string is not important because the infinitely thin tube of 2π flux can always be placed inside a halo of an underlying lattice and the unit flux can be gauged away. The gauge field in Eq. (7) represents an instanton with the Lorentz symmetry. In the presence of the nonrelativistic fermions, the space-time isotropy is lost and the field strength will be redistributed. With the broken Lorentz symmetry, the spatial rotational symmetry in the x_1-x_2 space may or may not be broken. In the following, we will first consider the case with

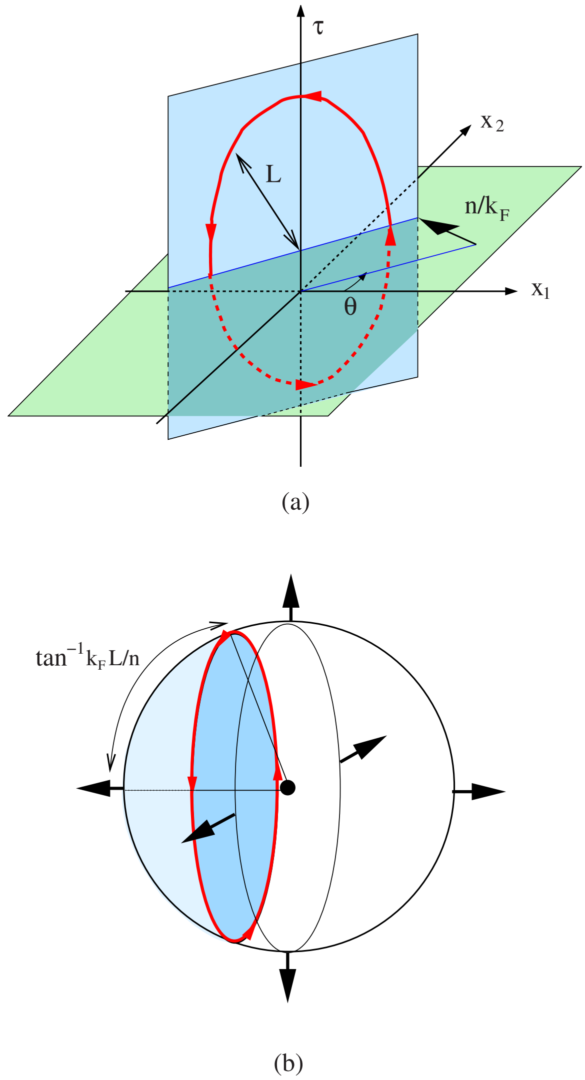

FIG. 2. (Color online) A 1+1D chiral fermion, which has an angular momentum n is coupled to a background gauge field projected to the plane that is represented as the vertical plane in (a). The arrowed circle in (a) is a trajectory of a fermion transported around an instanton at distance L and the arrowed circle in (b) is the trajectory of the fermion projected on the unit sphere. The area of the shaded region in (b) is the solid angle enclosed by the fermion around the instanton, which is represented as the black dot at the center of the sphere. In the large distance limit ($L \gg n/l_F$), the fermion acquires phase π as it moves around the instanton.

the spatial rotational symmetry and then consider general cases without the symmetry.

As a 1+1D fermion is transported within a plane at distance L from its origin as in Fig. 2(a), it encloses the solid angle, $\Omega_n(L)=2\pi[1-\frac{n}{\sqrt{(Lk_F)^2+n^2}}]$ in the unit sphere around the instanton as is shown in Fig. 2(b). Since an instanton is the source of flux 2π, the fermion acquires a nontrivial phase $\Phi_n(L)$. Without loss of generality, we can define the phase angle within the interval $(-\pi,\pi]$. For the Lorentz symmetric instanton configuration in Eq. (7), the phase angle is the half of the solid angle and becomes

$$\Phi_n(L) = \mathrm{sgn}(n)\pi\left[1 - \frac{|n|}{\sqrt{(Lk_F)^2+n^2}}\right]. \tag{8}$$

For nonisotropic configurations, $\Phi_n(L)$ will be different from Eq. (8). However, the explicit form of $\Phi_n(L)$ is not important for the following discussions. What is important is the fact that $|\Phi_n(L)| \to \pi$ for any finite n as $L\to\infty$ in the presence of the spatial rotational symmetry. This is because trajectories of fermions projected onto the unit sphere around the instanton will eventually follow a big circle for any angular momentum n in the large L limit and the flux enclosed by any half sphere that cuts through the north and south poles is always π due to the spatial rotational symmetry. Therefore, in the long-distance limit, an instanton twists the boundary conditions (BCs) of all fermions from the periodic condition to the antiperiodic one. Roughly speaking, at a length scale L, an instanton twists the boundary conditions of the fermions, which have angular momenta $|n| < k_F L$ by π.

Having understood that an instanton operator corresponds to a twist operator, we can determine the scaling dimension of instanton. To do this, we represent the 1+1D space in terms of a complex variable, $z=\tau - ix$, and rescale the fermion fields to write the action in the standard form,

$$S_{\mathrm{free}} = \frac{1}{2\pi}\sum_{j=1}^{N}\sum_{n=-\infty}^{\infty}\int dz d\bar{z}\ \ \psi^*_{jn}\bar{\partial}\psi_{jn}, \tag{9}$$

where $\bar{\partial}=\frac{\partial}{\partial\bar{z}}$. This free theory is invariant under the scale transformation,

$$z = bz',$$

$$\bar{z} = b\bar{z}',$$

$$\psi_{jn}(b\tau',bx') = b^{-1/2}\psi'_{jn}(\tau',x') \tag{10}$$

with $b>1$. With instantons, the free theory is perturbed as

$$S = S_{\mathrm{free}} + y\int dz d\bar{z}\ \ \sigma, \tag{11}$$

where σ is the creation operator of an instanton or an anti-instanton and y is the fugacity. Since an instanton twists the boundary conditions of all fermions in the low-energy limit, the instanton operator can be written as

$$\sigma = \Pi_{j,n}\sigma_{jn}(\pi), \tag{12}$$

where $\sigma_{jn}(\pi)$ is the operator, which twists the boundary condition of ψ_{jn} by π. However, the scaling dimension of σ is not well defined because the operator ends up twisting the infinite number of fermions by the finite angle, π. Actually, not all fermions are twisted by the same angle at a finite length scale L.[31] Therefore we introduce a regularized instanton operator,

$$\sigma_L = \Pi_{j,n}\sigma_{jn}[\Phi_n(L)], \tag{13}$$

where $\sigma_{jn}[\Phi_n(L)]$ is an operator that twists the boundary condition of ψ_{jn} by the angle $\Phi_n(L)$. Physically, σ_L creates the flux configuration near an instanton at a length scale L. Although σ_L is not a true instanton operator, we can learn about the property of the true instanton by taking $L\to\infty$ limit of σ_L. The point of introducing the regularized operator is that σ_L is a well defined local operator, which has a finite scaling dimension, as will be shown below.

Since the scaling dimension corresponds to the eigenvalue of the scale transformation generated by the Noether current $j_\nu = x^\mu T_{\mu\nu}$, the scaling dimension d_L of the regularized instanton operator can be obtained from

$$d_L\sigma_L(0) = \oint \frac{dz}{2\pi i} zT(z)\sigma_L(0), \qquad (14)$$

where $T(z)$ is the holomorphic energy-momentum tensor. In the state operator correspondence, we can view the scaling dimension as the "energy" of the quantum state defined on a circle around the origin associated with the "time" evolution in the radial direction. What the insertion of the σ_L operator does is to twist the boundary condition of ψ_{jn} by $\Phi_n(L)$. Then we can rewrite Eq. (14) as

$$d_L = \left\langle \oint \frac{dz}{2\pi i} zT(z) \right\rangle_{\text{twisted BC}}, \qquad (15)$$

where we impose the twisted boundary condition for the fermion fields around the origin. Each fermion ψ_{jn} contribute a scaling dimension $d[\Phi_n(L)] = \frac{\Phi_n(L)^2}{8\pi^2}$ (see Appendix A for the derivation) and the total scaling dimension for the regularized instanton operator becomes

$$d_L = \sum_{j=1}^{N}\sum_{n=-\infty}^{\infty} \frac{\Phi_n(L)^2}{8\pi^2}. \qquad (16)$$

Since $\Phi_n(L)$ approaches π as L increases, d_L diverges in the large L limit. For the isotropic instanton configuration, we have

$$d_L^{\text{isotropic}} = \sum_{j=1}^{N}\sum_{n=-\infty}^{\infty} \frac{1}{8}\left[1 - \frac{|n|}{\sqrt{(Lk_F)^2 + n^2}}\right]^2, \qquad (17)$$

and it is easy to check that it diverges linearly with L. The renormalization group equation for the fugacity becomes

$$\frac{dy_L}{d\ln b} = (2 - d_L)y_L + O(y_L^2), \qquad (18)$$

where y_L is the fugacity of the regularized instanton operator. The present approach does not allow us to calculate the higher-order terms in y. However, from the linear term alone, we can readily see that for any $N>0$ the regularized instanton operator for a sufficiently large L (hence the true instanton operator defined as $\sigma = \lim_{L\to\infty}\sigma_L$) is strongly irrelevant at the fixed point with $y=0$. Namely, a small nonzero y will flow to the fixed point with $y=0$. Although the scaling dimension of the true instanton operator defined as $d = \lim_{L\to\infty} d_L$ is ill defined (infinite) for any $N>0$, the regularized scaling dimension diverges more rapidly with increasing L when N is larger. This is consistent with the physical intuition that the presence of more fermions results in a larger scaling dimension of instanton via screening.

Until now, we have considered the case with the spatial rotational symmetry. If the symmetry is broken by an underlying lattice, the field configuration of an instanton is no longer symmetric under the spatial rotation. Here we will see that the conclusion reached for the rotationally symmetric Fermi surface holds in general cases too, as far as the general Fermi surface can be obtained from the symmetric one through a smooth deformation. Performing the Fourier transformations for the frequency and the radial momentum, we rewrite S_1 in Eq. (3) as

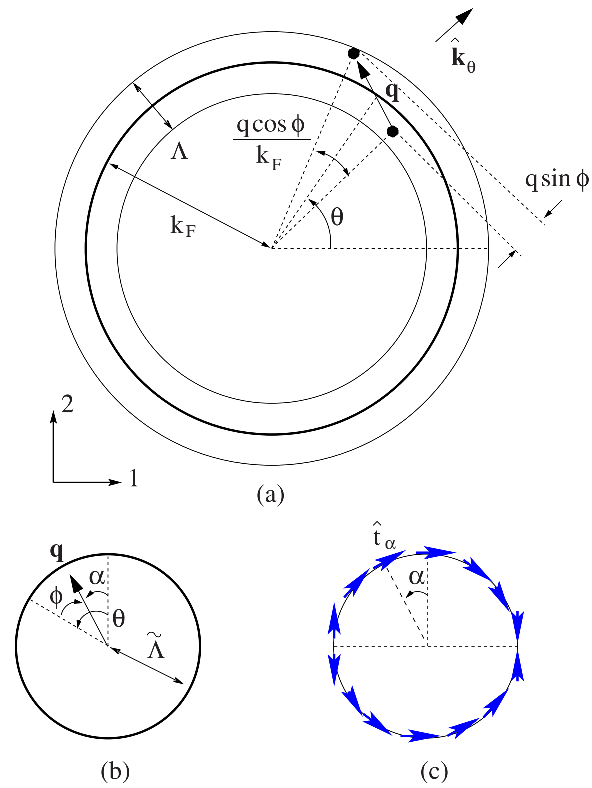

FIG. 3. (Color online) Angular representations of (a) the fermions and (b) the gauge field. Note that the angle θ for the fermions is measured from the x_1 axis and the angle α for the gauge field is measured from the x_2 axis so that the momentum of the gauge field becomes perpendicular to the Fermi momentum when $\alpha=\theta$. In (a), the arrow represents a process where a fermion changes its radial momentum and angle through an absorption of a momentum from the gauge field. In (b), ϕ parametrizes a deviation of α from θ. In (c), the arrows represent the polarization vectors of the transverse gauge field at different points in the momentum space.

$$S_1 = -\frac{1}{(2\pi)^{1/2}}\int d\tau dx d\theta d\theta' \; a_\theta[\tau,x,k_F(\theta-\theta');(\theta + \theta')/2]\psi_j^*(\tau,x,\theta)\psi_j(\tau,x,\theta'). \qquad (19)$$

For a general Fermi surface, a_θ has a nontrivial angular dependence on $(\theta+\theta')/2$. To diagonalize the action, we have to use a different basis than the angular momentum basis. We consider the basis transformation,

$$\psi_{jn}(\tau,x) = \frac{1}{(2\pi)^{1/2}}\int d\theta \; f_n^*(\tau,x,\theta)\psi_j(\tau,x,\theta), \qquad (20)$$

where $f_n(\tau,x,\theta)$ satisfies the eigenvalue equation,

$$\frac{1}{(2\pi)^{1/2}}\int d\theta' a_\theta[\tau,x,k_F(\theta-\theta');(\theta+\theta')/2]f_n(\tau,x,\theta') = a_n(\tau,x)f_n(\tau,x,\theta) \quad (21)$$

and the normalization condition,

$$\frac{1}{2\pi}\int d\theta f_m^*(\tau,x,\theta)f_n(\tau,x,\theta) = \delta_{m,n}. \quad (22)$$

One can always find such a basis because the kernel a_θ satisfies the Hermitian condition, $a_\theta[\tau,x,k_F(\theta-\theta');(\theta+\theta')/2] = a_\theta^*[\tau,x,-k_F(\theta-\theta');(\theta+\theta')/2]$, at each τ and x. In the basis, the action for the 1+1D chiral fermions becomes diagonal,

$$S = \sum_n \int d\tau dx \; \psi_{jn}^*(\tau,x)\{\partial_\tau - i[\partial_x - ia_n(\tau,x)]\}\psi_{jn}(\tau,x). \quad (23)$$

The phase acquired by the nth fermion when the fermion is transported around the instanton is

$$\Phi_n = \oint dx a_n, \quad (24)$$

and the total scaling dimension becomes

$$d = N\sum_n \frac{\Phi_n^2}{8\pi^2}, \quad (25)$$

where $-\pi<\Phi_n\leq\pi$. For the rotationally symmetric Fermi surface, the index n represents the angular momentum as before and $\Phi_n=\pi$ for all n in the low-energy limit. As the Fermi surface (hence the field configuration of an instanton) is distorted, the distribution of Φ_n gets broadened around $\pm\pi$ and d will decrease. However, d cannot change abruptly as the Fermi surface is smoothly deformed and d will remain infinite in the thermodynamic limit unless there is a phase transition associated with the topology of the Fermi surface. Therefore, the scaling dimension of an instanton is infinite for a general Fermi surface, as far as the Fermi surface is smoothly connected to the rotationally symmetric Fermi surface.

IV. INTERACTING FERMIONS WITH A LARGE NUMBER OF FLAVORS

Now we consider the whole theory by taking into account fluctuations of the noncompact gauge field. For the noncompact gauge field, we will use the Coulomb gauge, where $\nabla\cdot\mathbf{a}=0$ (Ref. 32), and drop the temporal gauge field, which is screened out at long distances. In the following, we will focus on the rotationally symmetric case. With the fluctuating noncompact gauge field, the interaction term can be written as

$$S_1 = \frac{-1}{(2\pi)^{3/2}}\int_{-\infty}^{\infty} d\omega \int_{-\Lambda/2}^{\Lambda/2} dk \int_{-\pi}^{\pi} d\theta \int_{-\infty}^{\infty} d\nu \int_0^{\tilde{\Lambda}} dq q \int_{-\pi}^{\pi} d\phi \Theta(\Lambda/2 - |k+q\sin\phi/2|)\Theta(\Lambda/2-|k-q\sin\phi/2|)\hat{k}_\theta\cdot\hat{t}_{\theta-\phi}a(\nu,q,\theta-\phi) \times \psi_j^*(\omega+\nu/2,k+q\sin\phi/2,\theta+q\cos\phi/2k_F)\psi_j(\omega-\nu/2,k-q\sin\phi/2,\theta-q\cos\phi/2k_F), \quad (26)$$

where a is the transverse gauge field. The momentum of the gauge field is also written in the polar coordinate as $a(\nu,q,\alpha)=a(\nu,q_1=-q\sin\alpha,q_2=q\cos\alpha)$. $\hat{t}_\alpha$ is the polarization vector of the gauge field with an angle α, where the angle is defined in such a way that $\hat{t}_\alpha$ becomes parallel to $\hat{k}_\theta$ when $\alpha=\theta$, as depicted in Fig. 3. We choose the polarization vector as $\hat{t}_\alpha=(\cos\alpha,\sin\alpha)$ for $-\pi/2\leq\alpha<\pi/2$ and $\hat{t}_\alpha=[\cos(\alpha+\pi),\sin(\alpha+\pi)]$ for $\alpha\geq\pi/2$ or $\alpha<-\pi/2$, as shown in 3(c). In this definition, there are discontinuities in $\hat{t}_\alpha$ at $\alpha=\pm\pi/2$. However, this definition is convenient in making the reality of the gauge field explicit in the momentum space as $a(-\nu,q,\alpha+\pi)=a^*(\nu,q,\alpha)$. $\Theta(x)$ is the step function, which ensures that the momenta of fermions lie within the shell of the width Λ near the Fermi surface.

At low energies we have $\tilde{\Lambda}\sim\sqrt{k_F\Lambda}$ because the Fermi surface is locally parabolic. Since $k_F\gg\tilde{\Lambda}\gg\Lambda$, typical momenta of the gauge field are perpendicular to fermion momentum and much larger than Λ. Therefore the support of the ϕ integration in Eq. (26) is sharply centered at $\phi=0$ and $\phi=\pi$ with the width of the order of $\Lambda/\tilde{\Lambda}\ll1$. This allows us to use $\sin\phi\approx\pm\phi$ and $\cos\phi\approx\pm1$ in the low-energy limit. Because both of the fermions with angles θ and $\theta+\pi$ are coupled with both of the gauge fields with angle θ and $\theta+\pi$, it is convenient to define two separate fields for the opposite moving fermions and to restrict the integrations of θ to run from $-\pi/2$ to $\pi/2$. At the same time, we allow q to run from $-\tilde{\Lambda}$ to $\tilde{\Lambda}$ and restrict the ϕ integration to $-\Lambda/|q|<\phi<\Lambda/|q|$ to implement the theta functions in Eq. (26). Then the action can be written as $S=S_0+S_1$, where

$$S_0 = \sum_{s=\pm1}\int_{-\infty}^{\infty} d\omega \int_{-\Lambda/2}^{\Lambda/2} dk \int_{-\pi/2}^{\pi/2} d\theta\,(i\omega + sk)\psi_{js}^*(\omega,k,\theta)\psi_{js}(\omega,k,\theta) + \int_{-\infty}^{\infty} d\nu \int_{-\tilde{\Lambda}}^{\tilde{\Lambda}} dq|q| \int_{-\pi/2}^{\pi/2} d\alpha \left[\frac{1}{2g^2}(\nu^2+q^2) + K\right]a(\nu,q,\alpha)a(-\nu,-q,\alpha), \quad (27)$$

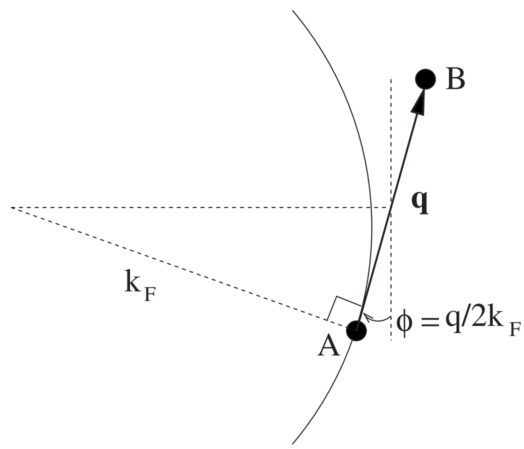

FIG. 4. The effect of the local curvature in the Fermi surface. As a fermion with a momentum A on the Fermi surface absorbs a momentum $\mathbf{q}$, which is tangential to the Fermi surface at the point, the fermion ends up with the momentum B, which has a higher energy by $q^2/2k_F$ due to the curvature of the Fermi surface. This can be seen from Eq. (28) as follows: In order for $\mathbf{q}$ to be tangential to the Fermi surface at the initial momentum, ϕ in Eq. (28) has to be $q/2k_F$. Then the energy of the final state is larger than that of the initial state by $q\phi = q^2/2k_F$.

$$S_1 = -\sum_{s=\pm 1}\frac{1}{(2\pi)^{3/2}}\int_{-\infty}^{\infty}d\omega\int_{-\Lambda/2}^{\Lambda/2}dk\int_{-\pi/2}^{\pi/2}d\theta\int_{-\infty}^{\infty}d\nu\int_{-\tilde{\Lambda}}^{\tilde{\Lambda}}dq|q| \times\int_{-\Lambda/|q|}^{\Lambda/|q|}d\phi\, s a(\nu,q,\theta-\phi)\psi_{js}^{*}(\omega+\nu/2,k+q\phi/2,\theta + sq/2k_F)\psi_{js}(\omega-\nu/2,k-q\phi/2,\theta-sq/2k_F), \quad (28)$$

where $s=1,-1$ labels the fermion fields on the two sides of the Fermi surface at each angle $-\pi/2 \leq \theta < \pi/2$, defined as

$$\psi_{j+}(\omega,k,\theta) = \psi_j(\omega,k,\theta),$$

$$\psi_{j-}(\omega,k,\theta) = \psi_j[\omega,-k,-\text{sgn}(\theta)\pi+\theta], \quad (29)$$

and a negative q of the gauge field represents the opposite momentum as

$$a(\nu,-|q|,\alpha) = a(\nu,|q|,\alpha+\pi) \quad (30)$$

with $-\pi/2 \leq \alpha < \pi/2$. ψ_{j+} and ψ_{j-} have the opposite velocities and form a two component $1+1$D Dirac fermion.

The present approach is conceptually analogous to the bosonized descriptions of Fermi surface,[33–36] where chiral bosons describe low-energy particle-hole excitations near Fermi surface. However, there is an important difference. In the previous bosonized description of the Fermi surface coupled with the U(1) gauge field,[36] the Fermi surface is taken to be locally flat within each momentum patch and the local curvature is not taken into account. The present formalism captures the local curvature effect of the Fermi surface, which is important in reproducing correct low-energy behaviors.[21] The key is to consider all points on the Fermi surface on the equal footing, not treating the Fermi surface as a sum of locally flat Fermi segments. The way the curvature effect is implemented in Eq. (28) is explained in Fig. 4.

Here we assume that $N \gg 1$ in which case the fluctuations of the gauge field are controlled. In the leading order of the $1/N$ expansion, vertex corrections can be ignored.[19] The fluctuating gauge field and the gapless fermions lead to singular self-energies and the single-particle quantum effective action of the fermions and the transverse gauge field becomes (see Appendix B)

$$\Gamma_0 = \sum_{s=\pm 1}\int d\omega dk d\theta[ic\,\text{sgn}(\omega)|\omega|^{2/3} + sk]\psi_{js}^{*}(\omega,k,\theta)\psi_{js}(\omega,k,\theta) + \int d\nu dq|q|d\alpha\left[\gamma\frac{|\nu|}{|q|}+\chi q^2\right]a^{*}(\nu,q,\alpha)a(\nu,q,\alpha), \quad (31)$$

where c, γ, and χ are constants. Because of the singular quantum corrections, the scaling transformation in Eq. (10) is no longer a symmetry. Instead, we have to rescale energy and momentum as

$$\omega = b^{-1}\omega',$$

$$\nu = b^{-1}\nu',$$

$$\Lambda = b^{-2/3}\Lambda',$$

$$\tilde{\Lambda} = b^{-1/3}\tilde{\Lambda}',$$

$$k = b^{-2/3}k',$$

$$q = b^{-1/3}q'. \quad (32)$$

Note that the momentum of the fermion in the radial direction and the momentum of the gauge field should scale differently. If we apply this new scale transformation to S_1 in Eq. (28), we readily notice that the action cannot be made invariant unless the angular variables θ and ϕ are rescaled as well. This is because the momenta of the fermions and the gauge field mix with the angular variables through $k+q\phi$ and $\theta+sq/k_F$. To make the action invariant, we should assign the scaling dimension 1/3 to the angular variables. This is an anomalous scaling dimension of the angular variables, which arises solely from quantum effects. The whole action is invariant if we rescale,

$$\theta = b^{-1/3}\theta',$$

$$\phi = b^{-1/3}\phi',$$

$$\psi_a(b^{-1}\omega',b^{-2/3}k',b^{-1/3}\theta') = b^{4/3}\psi_a'(\omega',k',\theta'),$$

$$a(b^{-1}\nu',b^{-2/3}q',b^{-1/3}\phi') = b^{4/3}a'(\nu',q',\phi'), \quad (33)$$

along with Eq. (32). As we go to lower energy ($b>1$), the range of the θ integration increases from $(-\pi/2,\pi/2)$ to $(-b\pi/2,b\pi/2)$. In the low-energy limit where $b\to\infty$, θ becomes a noncompact variable that runs from $-\infty$ to ∞. The physical reason behind this "decompactification" of the an-

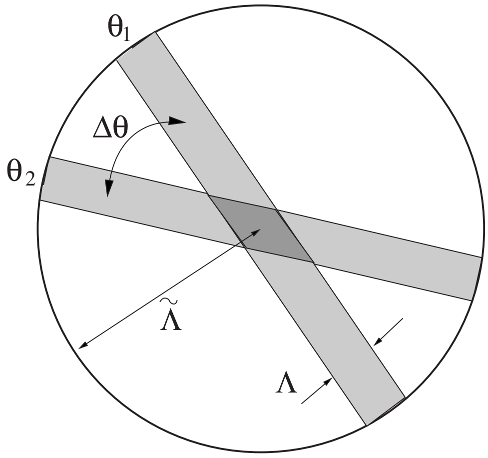

FIG. 5. The shaded areas with angles θ_1 and θ_2 represent momentum points, which are included in $a_q(\tau,x,\theta_1)$ and $a_q(\tau,x,\theta_2)$. The dark region at the center indicate momentum points, which contribute to both $a_q(\tau,x,\theta_1)$ and $a_q(\tau,x,\theta_2)$. The ratio of the area of the dark region to the area of a strip becomes zero in the low-energy limit where the momentum cutoffs scale as $\Lambda \to b^{-2/3}\Lambda$ and $\tilde{\Lambda} \to b^{-1/3}\tilde{\Lambda}$.

gular variable can be understood in the following way. In the low-energy limit, the gauge field becomes more and more ineffective in scattering fermions from one momentum to another momentum along the tangential directions to the Fermi surface. This is because the momentum of the gauge field is scaled down under the scale transformation while the circumference of the Fermi surface is unchanged. This effectively makes two momentum points on the Fermi surface more decoupled from each other at lower energies. In other words, the "metric" of the Fermi surface along the tangential directions diverges in the low-energy limit compared to the metric along the perpendicular directions.

Introducing $1+1$D fields in real space,

$$\psi_{js}(\tau,x,\theta) = \frac{1}{2\pi}\int_{-\infty}^{\infty} d\omega \int_{-\Lambda/2}^{\Lambda/2} dk \;\; e^{i(\omega\tau + kx)}\psi_{js}(\omega,k,\theta), \tag{34}$$

$$a_q(\tau,x,\theta) = \frac{1}{2\pi}\int_{-\infty}^{\infty} d\omega \int_{-\Lambda/|q|}^{\Lambda/|q|} d\phi |q| \;\; e^{i(\omega\tau + xq\phi)}a(\omega,q,\theta-\phi), \tag{35}$$

we can write down the low-energy effective action in the $1+1$D real space as

$$S = \sum_{s=\pm1}\int d\tau dx d\theta \;\; \psi^*_{js}(\tau,x,\theta)[\partial_\tau - is\partial_x]\psi_{js}(\tau,x,\theta) + \frac{1}{2\Lambda}\int d\tau dx d\theta dq \;\; |q| a^*_q(\tau,x,\theta)\left(\frac{1}{2g^2}(-\partial_\tau^2 + q^2) + K\right)a_q(\tau,x,\theta) - \frac{1}{(2\pi)^{1/2}}\sum_{s=\pm1}\int d\tau dx d\theta dq \;\; s a_q(\tau,x,\theta)\psi^*_{js}(\tau,x,\theta + sq/2k_F)\psi_{js}(\tau,x,\theta - sq/2k_F). \tag{36}$$

It should be emphasized that in this action θ is a noncompact variable, which runs from $-\infty$ to ∞. In Eq. (35), $a_q(\tau,x,\theta)$ depends on four variables while $a(\omega,q,\theta-\phi)$ depends only on three independent variables. The variable x has been created by the Fourier transformation of $a(\omega,q,\alpha)$ with respect to α, which is centered at θ. Conceptually, this is similar to creating a wave packet, which is localized in both real space and momentum space by linearly superposing wave functions whose momenta are centered at a particular momentum. The factor $1/2\Lambda$ in the second line of Eq. (36) is to cancel the double counting of momentum points. Note that $a_q(\tau,x,\theta_1)$ and $a_q(\tau,x,\theta_2)$ are not completely independent for different θ_1 and θ_2. Both $a_q(\tau,x,\theta_1)$ and $a_q(\tau,x,\theta_2)$ include contributions from a common region in the momentum space, as shown in Fig. 5. However, the overlap is not important in determining the scaling dimension of instanton as will be shown in the following. The area of the common region for $a_q(\tau,x,\theta_1)$ and $a_q(\tau,x,\theta_2)$ (the dark parallelogram in Fig. 5) is $(\Lambda^2/\Delta\theta)$ for a small $\Delta\theta = \theta_2 - \theta_1$. The ratio of this area to the area included in $a_q(\tau,x,\theta)$ (the long strip in Fig. 5) is $\gamma = (\Lambda^2/\Delta\theta)/(\Lambda\tilde{\Lambda})$. As the momentum cutoff decreases as $\Lambda \to \Lambda b^{-2/3}$ and $\tilde{\Lambda} \to \tilde{\Lambda} b^{-1/3}$, the ratio decreases as $\gamma \to b^{-1/3}(\Lambda/\tilde{\Lambda}\Delta\theta)$. The ratio becomes zero in the low-energy limit for any nonzero $\Delta\theta$, which implies that the two fields that have a finite angle difference (before scaling) are independent in the low-energy limit. In the rescaled angular variable $\theta' = b^{1/3}\theta$, a fixed $\Delta\theta'$ corresponds to a successively reduced $\Delta\theta = b^{-1/3}\Delta\theta'$ as a low-energy limit is taken. Since γ goes as b^0 for a fixed $\Delta\theta'$ in the rescaled variable, two fields, which have a fixed angle different $\Delta\theta'$, have a finite ratio γ in the low-energy limit. On the other hand, two fields whose angle difference increases faster than $\Delta\theta' = b^0$ in the rescaled variable have vanishing overlap in the low-energy limit. Since the interval of θ' increases as $b^{1/3}\pi$, there are infinitely many independent fields $a_q(\tau,x,\theta)$, which are separated in the angular direction and have only local interactions. We call this property an asymptotic locality. This will play a crucial role in determining the scaling dimension of instanton as will be discussed later.

Now we can determine the scaling dimension of the instanton operator. At a scale set by τ and x, fermion modes whose angular momenta are less than $n_{\max} \sim k_F \min(x,\tau) = k_F x$ are twisted (at sufficiently large distances, we always have $\tau > x$ because space has the smaller absolute scaling dimension). In other words, fermion fields that are twisted at scale x have "wavelengths" larger than $\delta\theta \sim 1/n_{\max} \sim (k_F x)^{-1}$ in the space of θ. Since x and θ scale as $x = b^{2/3}x'$ and $\theta = b^{-1/3}\theta'$, we have $\delta\theta' \sim b^{-1/3}(k_F x')^{-1}$. Note that $\delta\theta' \to 0$ as $b \to \infty$ and fermion fields with arbitrarily small wavelengths are twisted in the low-energy limit. Since an instanton twists fermions of all angle, an instanton corresponds to an operator, which creates a vortex with flux π along the noncompact angle direction θ. The physical reason

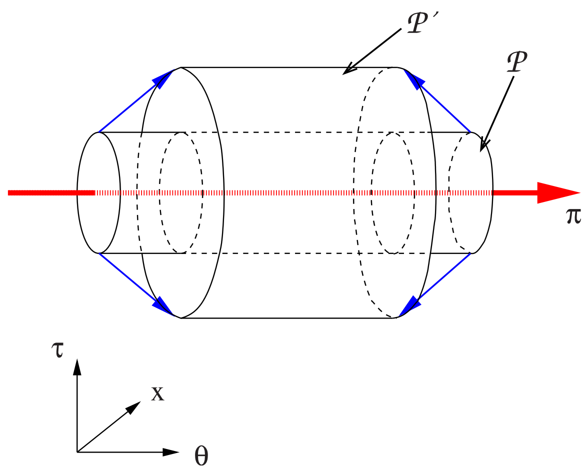

FIG. 6. (Color online) Time evolution of a quantum state defined on the surface of a pipe extended along the angular direction, where a π vortex is pierced through the pipe. Under the time evolution, a point on the surface $\mathcal{P}$ is mapped to a point on the surface $\mathcal{P}'$.

why an instanton, which is localized in space and in time, becomes an extended object is as follows: In the low-energy limits, only small-angle scatterings are important and fermions rarely change the directions of their motions. They essentially move on 1+1D planes in space and in time. Since the distances from the instanton and the planes on which fermions move are fixed, at a sufficiently large distance scale, all the fermions acquire phase π as they are transported around the instanton. The 1+1D fermions are parametrized by the direction of their velocities, θ, and an instanton becomes a vortex, which is extended along the angular direction.

It is noted that even though the (Euclidean) Lorentz symmetry is broken by the nonrelativistic fermions, the twist angle will be π in the long-distance limit if there is a spatial rotational symmetry as discussed in Sec. III. If there is no spatial rotational symmetry, the twist angle will depend on θ. However an argument similar to the one provided at the end of Sec. III can be made to extend the conclusion of the following discussion to more general cases. In the following, we will focus on the rotationally symmetric case.

The scaling dimension of the extended twist operator can be obtained by following the reasoning that is analogous to the state operator correspondence in relativistic quantum-field theories. In relativistic cases, instanton corresponds to an operator defined at a point in space and in time. The operator defines a quantum state on the sphere enclosing the instanton operator. The scaling dimension corresponds to the energy of the quantum state associated with the time evolution in the radial direction. In the present nonrelativistic case, instanton corresponds to an extended vortex operator with flux π because instanton twists the boundary conditions of all fermions, which are parametrized by the noncompact variable θ. The extended operator defines a quantum state on the surface of a pipe $\mathcal{P}$, which is extended in the θ direction in the space of τ, x, and θ, as shown in Fig. 6. In the functional Schrodinger picture, the vortex operator defines a quantum state as

$$\Psi[\psi'_{js}(\tau,x,\theta),\psi^{*\prime}_{js}(\tau,x,\theta),a'_q(\tau,x,\theta)]|_{(\tau,x,\theta)\in\mathcal{P}} = \int D\psi_{js}D\psi^*_{js}Da_q e^{-S[\psi,\psi^*,a]}. \quad (37)$$

On the right-hand side of the above equation, the fermion fields have the antiperiodic boundary condition and all the fields inside the pipe are integrated out with the condition that the fields on the surface of the pipe coincides with the fields $\psi'_{js}(\tau,x,\theta),\psi^{*\prime}_{js}(\tau,x,\theta),a'_q(\tau,x,\theta)$. The scaling dimension corresponds to the energy of this quantum state associated with the time evolution given by

$$x\rightarrow b^{2/3}x,$$

$$\tau\rightarrow b^{1}\tau,$$

$$\theta\rightarrow b^{-1/3}\theta. \quad (38)$$

We can define the Hamiltonian for time evolution because the action is local in τ and x. Namely, a quantum state on a surface with larger $|\tau'|$ and $|x'|$ are uniquely determined from the state on a surface with smaller $|\tau|$ and $|x|$.

Since τ and x scale differently, the surface of the pipe should expand in different rates depending on its normal vector. Note that the time evolution also involves the transformation in θ because of the anomalous dimension of the angular variable. In determining the scaling dimension of instanton, the key is the locality of the action in the angular variable θ. The action Eq. (36) is asymptotically local in the space of θ in the following senses: First, angles of the fermions can change at most by $\tilde{\Lambda}/k_F$ through an interaction with the gauge field. Second, the fermion field at angle θ is coupled only with the gauge field near angle θ. Third, two gauge fields, which have different angles θ_1 and θ_2, are independent for a sufficiently large $|\theta_2-\theta_1|$, which is, yet, much smaller than the range of the θ. One may worry about a possible breakdown of the locality in the angular direction in the presence of short-range four fermion interactions. Indeed, the four fermion interactions:

$$V\int \Pi_{i=1}^4 d\omega_i dk_i d\theta_i \;\; \psi^*(\omega_1,k_1,\theta_1)\psi^*(\omega_3,k_3,\theta_3),$$

$$\psi(\omega_2,k_2,\theta_2)\psi(\omega_4,k_4,\theta_4)\delta\left[\sum_i(-1)^i\omega_i\right],$$

$$\delta\left[\sum_i(-1)^i(k_F+k_i)\cos\,\theta_i\right]\delta\left[\sum_i(-1)^i(k_F+k_i)\sin\,\theta_i\right], \quad (39)$$

are nonlocal in the angular direction. However, the interaction strength scales as $V\rightarrow b^{-2/3}V$ under the transformations in Eqs. (32) and (33) and the four fermion interaction is irrelevant at low energies.

Because of this locality of the action, any extended object should have an energy that is either zero or infinite with respect to the vacuum. This is a very general statement for a local theory. For example, if a local theory is defined in a range $0<\theta<2L$, where L is much larger than any length scale of the local coupling in the theory, the energy of the system is roughly twice the energy of the system defined in the range $0<\theta<L$. This implies that only zero or $\pm\infty$ are possible for the energy of the vortex operator with respect to the vacuum energy. The vortex is a nontrivial object, which necessarily "excites" the fermionic state by twisting the boundary condition, and it should have an infinite energy. Note that $-\infty$ (zero) are excluded because a negative (zero) energy would imply that instanton becomes more relevant (equally relevant) with increasing number of spinon flavors or with increasing length of Fermi surface in the momentum space. This is unlikely because the fermions always screen the gauge field and the scaling dimension of instanton should increase as the number of fermion modes increases. Although the scaling dimension defined in the thermodynamic limit is infinite, the scaling dimension of the regularized instanton operator is well defined and systematically increases as the number of available fermion modes increases. The number of fermion modes in a finite system is proportional to the number of spinon flavors and the length of the Fermi surface due to a finite mesh in the momentum space. This implies that the scaling dimension of the instanton operator diverges more rapidly as the long-distance limit is taken when there are more flavors or longer Fermi surface. An explicit example of this is provided in Eqs. (16) and (17) for the noninteracting system, where the scaling dimension of the regularized instanton operator increases as N or k_F increases. Therefore we conclude that instanton has to have a positive infinite scaling dimension in general.

V. STRONGLY INTERACTING FERMIONS WITH FEW FLAVORS

Now we move on to the physical case with a small but nonzero N, e.g., $N=2$. In this case, even if one can somehow ignore instantons, the fermions are already strongly coupled with the noncompact gauge field. Therefore, one cannot exclude the possibility that the strongly interacting fixed point becomes unstable against a particle-hole or particle-particle condensation[21,37,38] due to the strongly fluctuating noncompact gauge field. Here we set aside those possibilities caused by the noncompact gauge field and focus on the question whether the fixed point is stable against proliferation of instantons or not. Because we cannot ignore vertex corrections anymore, we do not know what the precise form of the scale transformation is for the strongly interacting fixed point. However, we can still argue that the scaling dimension of an instanton is infinite based on the locality of the low-energy theory in the angular direction. The emergence of the locality in the angular direction is independent of a particular form of scale transformation. Because of the Fermi-surface geometry, momentum of the gauge field should be scaled down more slowly compared to radial momentum of the fermions. If a momentum of fermion scales as $k=b^{-a}k'$, then a momentum of the gauge field should scale as $q=b^{-a/2}q'$, which is the consequence of the fact that Fermi surface is locally parabolic unless there is a nesting that we do not consider here. Therefore, we have $q/k \gg 1$ at low energies and this forces fermions at a certain angle are coupled only with the gauge field whose momentum is tangent to the Fermi surface. This guarantees that the low-energy effective action should be local in the angular direction. Moreover, the mixing between k and q gives rise to the anomalous scaling dimension for the angular variable, $a/2>0$, and the angular variable becomes decompactified in the low-energy limit. Again, this implies that the instanton operator is an extended vortex with flux π along the extended angular direction. Because of the locality, the extended vortex should have an infinite scaling dimension as we have discussed previously.

VI. CONCLUSION

In conclusion, we argue that the U(1) spin liquid state is stable against proliferation of instantons for any nonzero number of spinon flavors if there is a spinon Fermi surface. We formulated the low-energy modes near the Fermi surface in terms of an infinite set of chiral fermions and made an observation that the angular variable that parametrize the Fermi surface acquires a positive scaling dimension due to quantum effects and becomes a noncompact variable in the low-energy limit. Because the low-energy effective theory is local in the noncompact angular direction, an instanton, which twists the boundary conditions of all chiral fermions, should have an infinite scaling dimension. Therefore, instantons are strongly irrelevant and the noncompact U(1) gauge theory is a good low-energy description.

A few comments are in order. First, since the scaling dimension of instanton is infinite in the infrared limit, a small fugacity of instantons will rapidly flow to zero at low energies. A finite fugacity at an intermediate length scale implies that there is a small but finite density of instantons at the length scale. However, the renormalization group flow implies that the density at a larger distance scale will become smaller and instantons are not important in a long-distance limit. If the fugacity y is tuned to a sufficiently large value via tuning some microscopic parameters, then the nonlinear terms in the flow equation, Eq. (18), becomes important and the sum of them may not converge. This signifies a breakdown of the perturbative expansion, which is valid within a finite domain near the $y=0$ point. If this happens, the fugacity of the instanton operator can flow toward a large value leading to a confinement, despite the fact that the linear term has a large negative coefficient. It is noted that the infinite scaling dimension of instanton at the deconfined fixed point $y=0$ does not necessarily imply that the confinement phase is always unstable. Both the deconfinement and the confinement phases may have finite regions of stability in the parameter space, separated by a phase transition. To understand the nature of the confinement phase is an important open problem.[39] Second, we expect that the present argument can be generalized to the cases where there is no rotational symmetry or there are only segments of Fermi surface. This was demonstrated for the free fixed point at the end of Sec. III. We expect that the similar argument will also hold true at the interacting fixed point. This is because any finite segment of Fermi surface contains an infinite number of modes, which contribute to the scaling dimension of instanton.

ACKNOWLEDGMENTS

This work was supported by NSERC. The author thanks Matthew Fisher, Yong Baek Kim, Subir Sachdev and Xiao-Gang Wen for the helpful discussions and, particularly, Patrick Lee for the helpful comments and suggestions to improve the paper.

APPENDIX A: SCALING DIMENSION OF A GENERAL TWIST OPERATOR

Here we calculate the scaling dimension of a generalized twist operator. Let us suppose that the boundary condition of a fermion is twisted by an arbitrary angle around the twist operator, which is inserted at the origin. The fermion satisfies the twisted boundary condition,

$$\psi(ze^{2\pi i}) = e^{i\Phi}\psi(z), \tag{A1}$$

in the complex plane with $z=\tau-ix$, where $\Phi=2\pi(1/2-\eta)$ with $0\leq\eta<1$. $\eta=1/2$ corresponds to the untwisted periodic boundary condition and $\eta=0$ corresponds to the antiperiodic boundary condition. A general value of η between zero and one corresponds to a fermion twisted by a phase angle between $-\pi$ and π. The twisted boundary condition is implemented by the mode expansion,

$$\psi(z) = \sum_n \frac{\psi^{n+\eta}}{z^{n+\eta+1/2}},$$

$$\psi^*(z) = \sum_n \frac{\psi^{*n-\eta}}{z^{n-\eta+1/2}}, \tag{A2}$$

where $\psi^{n+\eta}$ and $\psi^{*n-\eta}$, with integer n, are the nth normal modes. Note that ψ and ψ^* have the different mode expansions because the gauge invariant operator $\psi^*\psi$ always have to satisfy the untwisted periodic boundary condition. The scaling dimension of the twist operator is given by

$$d = \left\langle \oint \frac{dz}{2\pi i} zT(z) \right\rangle_{\text{twisted BC}}, \tag{A3}$$

where the contour of the integration encloses the origin and

$$T(z) = \frac{1}{2}:[(\partial\psi^*)\psi - \psi^*\partial\psi]: \tag{A4}$$

is the regularized holomorphic energy-momentum tensor with

$$:\psi^*(z)\,\partial\psi(z):\equiv \lim_{w\to z}\left[\psi^*(w)\,\partial\psi(z) + \frac{1}{(w-z)^2}\right]. \tag{A5}$$

To calculate $\langle T(z)\rangle_{\text{twisted BC}}$, we first consider the expectation value of a fermion bilinear with the twisted boundary condition,

$$\langle\psi^*(w)\psi(z)\rangle_{\text{twisted BC}} = \sum_{m,n}\left\langle \frac{\psi^{m-\eta *}}{w^{m+1/2-\eta}}\frac{\psi^{n+\eta}}{z^{n+1/2+\eta}}\right\rangle = \frac{w^{\eta-1/2}z^{-\eta+1/2}}{w-z}, \tag{A6}$$

where we have used the commutator $\{\psi^{m-\eta\dagger},\psi^{n+\eta}\}=\delta_{m,-n}$ and the property of the vacuum, $\psi^{n+\eta}|0\rangle=\psi^{n-\eta\dagger}|0\rangle=0$ for $n>0$.[40] From Eqs. (A4)–(A6), we obtain

$$\langle T(z)\rangle_{\text{twisted BC}} = \frac{(2\eta-1)^2}{8z^2}, \tag{A7}$$

and from Eq. (A3) the scaling dimension is obtained to be $(2\eta-1)^2/8$. In the presence of multiple fermions, the total energy-momentum tensor is the sum of the individual energy-momentum tensors and the scaling dimension is the sum of the individual scaling dimensions. If the ith fermion is twisted by an angle Φ_i, the scaling dimension of the twist operator becomes

$$d = \sum_i \frac{\Phi_i^2}{8\pi^2}. \tag{A8}$$

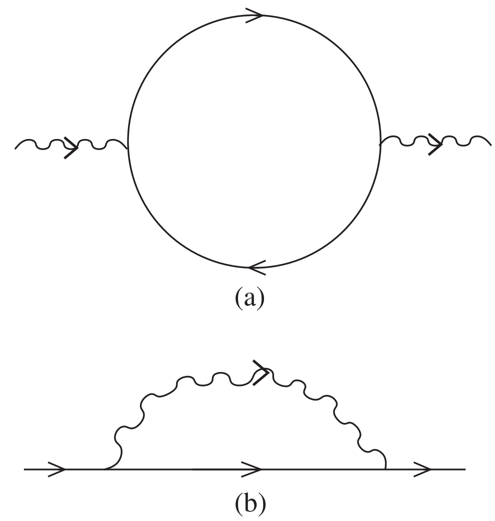

FIG. 7. Feynman diagrams for the one-loop self-energies of (a) the gauge field and (b) the fermions. The solid (wiggled) line represents the propagator of the fermions (gauge field).

APPENDIX B: CALCULATION OF THE SELF-ENERGIES

In the large N limit, the vertex corrections are negligible and the one-loop corrections are dominant.[19] Although the one-loop self-energies of the fermions and the gauge field are well known,[19–21] it is instructive to calculate them from the effective action Eqs. (27) and (28) to make sure that the theory contains the essential low-energy physics.

From the quadratic action in Eq. (27), the propagator of the fermion is given by

$$\langle\psi_{js}(\omega,k,\theta)\psi^*_{j's'}(\omega',k',\theta')\rangle = \delta_{jj'}\delta_{s,s'}\delta(\omega-\omega')\delta(k-k')\delta(\theta-\theta')g_s(\omega,k,\theta), \tag{B1}$$

where $g_s(\omega,k,\theta)=\frac{1}{i\omega+sk}$, and the propagator of the gauge field is given by

$$\langle a(\nu,q,\alpha)a(\nu',q',\alpha')\rangle = \frac{1}{|q|}\delta(\nu+\nu')\delta(q+q')\delta(\alpha - \alpha')\mathcal{D}_0(\omega,q,\alpha), \quad \text{(B2)}$$

where $\mathcal{D}_0(\nu,q,\alpha)=\frac{1}{\frac{1}{g^2}(\nu^2+q^2)+2K}$. The unconventional factor, $1/|q|$ in the gauge propagator is due to the angular representation.

Applying the standard Feynman rule to the action in Eq. (28), we can calculate the self-energy of the gauge field [Fig. 7(a)] as

$$\Pi(\nu,q,\alpha) = \frac{Nk_F}{(2\pi)^3}\sum_s \int d\omega dk d\phi, \quad g_s(\omega+\nu/2,k+q\phi/2,\phi + \alpha + sq/2k_F)g_s(\omega-\nu/2,k-q\phi/2,\phi+\alpha - sq/2k_F) = -\frac{Nk_F}{2\pi} + \frac{Nk_F}{4\pi}\frac{|\nu|}{|q|} \quad \text{(B3)}$$

for $|q| \gg |\nu|$. The dressed gauge propagator becomes

$$\mathcal{D}^{-1}(\nu,q,\theta-\phi) = \left(2K - \frac{Nk_F}{2\pi}\right) + \gamma\frac{|\nu|}{|q|} + \chi q^2, \quad \text{(B4)}$$

where γ and χ are the constants. The first term should be canceled due to the gauge invariance. The diamagnetic term K depends on the details of the high-energy cutoff (regularization) scheme, and we fix its value by requiring the gauge invariance. From Fig. 7(b), we obtain the self-energy of the fermions as

$$\Sigma_s(\omega,k,\theta) = -\frac{1}{(2\pi)^3}\int d\nu dq|q|d\phi \mathcal{D}(\nu,q,\theta-\phi)g_s(\omega-\nu,k - q\phi,\theta - sq/k_F), \quad \text{(B5)}$$

where it is essential to use the dressed gauge propagator,

$$\mathcal{D}(\nu,q,\alpha) = \frac{1}{\gamma|\nu|/|q| + \chi q^2}. \quad \text{(B6)}$$

The integration can be done straightforwardly, and we obtain,

$$\Sigma_s(\omega,k,\theta) = ic \ \mathrm{sgn}(\omega)|\omega|^{2/3}, \quad \text{(B7)}$$

where $c \sim \gamma^{-1/3}\chi^{-2/3}$ is a constant. Even though we use the dressed fermion propagator, the leading behaviors of the self-energies are not modified.[19]

[1] F. D. M. Haldane, J. Phys. C **14**, 2585 (1981).
[2] R. B. Laughlin, Phys. Rev. Lett. **50**, 1395 (1983).
[3] P. W. Anderson, Science **235**, 1196 (1987); P. Fazekas and P. W. Anderson, Philos. Mag. **30**, 423 (1974).
[4] P. A. Lee, N. Nagaosa, and X.-G. Wen, Rev. Mod. Phys. **78**, 17 (2006), and references therein.
[5] X.-G. Wen, Phys. Rev. B **65**, 165113 (2002).
[6] M. A. Levin and X.-G. Wen, Phys. Rev. B **67**, 245316 (2003); **71**, 045110 (2005); M. A. Levin and X.-G. Wen, Rev. Mod. Phys. **77**, 871 (2005).
[7] S.-S. Lee and P. A. Lee, Phys. Rev. B **72**, 235104 (2005).
[8] T. Senthil and P. A. Lee, Phys. Rev. B **71**, 174515 (2005).
[9] Y. Shimizu, K. Miyagawa, K. Kanoda, M. Maesato, and G. Saito, Phys. Rev. Lett. **91**, 107001 (2003).
[10] J. S. Helton, K. Matan, M. P. Shores, E. A. Nytko, B. M. Bartlett, Y. Yoshida, Y. Takano, A. Suslov, Y. Qiu, J.-H. Chung, D. G. Nocera, and Y. S. Lee, Phys. Rev. Lett. **98**, 107204 (2007).
[11] O. I. Motrunich, Phys. Rev. B **72**, 045105 (2005).
[12] S.-S. Lee and P. A. Lee, Phys. Rev. Lett. **95**, 036403 (2005).
[13] Y. Ran, M. Hermele, P. A. Lee, and X.-G. Wen, Phys. Rev. Lett. **98**, 117205 (2007).
[14] T. Senthil, M. Vojta, and S. Sachdev, Phys. Rev. B **69**, 035111 (2004).
[15] O. I. Motrunich and M. P. A. Fisher, Phys. Rev. B **75**, 235116 (2007).
[16] W. Rantner and X.-G. Wen, Phys. Rev. Lett. **86**, 3871 (2001); Phys. Rev. B **66**, 144501 (2002).
[17] P. A. Lee and N. Nagaosa, Phys. Rev. B **46**, 5621 (1992).
[18] B. I. Halperin, P. A. Lee, and N. Read, Phys. Rev. B **47**, 7312 (1993).
[19] J. Polchinski, Nucl. Phys. B **422**, 617 (1994).
[20] Y. B. Kim, A. Furusaki, X.-G. Wen, and P. A. Lee, Phys. Rev. B **50**, 17917 (1994).
[21] B. L. Altshuler, L. B. Ioffe, and A. J. Millis, Phys. Rev. B **50**, 14048 (1994).
[22] A. M. Polyakov, Phys. Lett. **59B**, 82 (1975); Nucl. Phys. B **120**, 429 (1977).
[23] M. Hermele, T. Senthil, M. P. A. Fisher, P. A. Lee, N. Nagaosa, and X.-G. Wen, Phys. Rev. B **70**, 214437 (2004).
[24] L. B. Ioffe and A. I. Larkin, Phys. Rev. B **39**, 8988 (1989).
[25] N. Nagaosa, Phys. Rev. Lett. **71**, 4210 (1993).
[26] I. Ichinose, T. Matsui, and M. Onoda, Phys. Rev. B **64**, 104516 (2001).
[27] I. F. Herbut, B. H. Seradjeh, S. Sachdev, and G. Murthy, Phys. Rev. B **68**, 195110 (2003).
[28] K.-S. Kim, Phys. Rev. B **72**, 245106 (2005).
[29] R. K. Kaul, S. Sachdev, and C. Xu, Phys. Rev. B **78**, 045110 (2008).
[30] R. Shankar, Rev. Mod. Phys. **66**, 129 (1994).
[31] The fact that the twist angles saturate to π only in the large L limit is due to the nonlocal nature of the instanton operator.
[32] It is convenient to choose the temporal gauge for the singular part and the Coulomb gauge for the nonsingular part. Note that it is possible to choose different gauges for singular and nonsingular parts.
[33] F. D. M. Haldane, in *Perspectives in Many-Particle Physics*, edited by R. Broglia and J. R. Schrieffer (North-Holland, Amsterdam, 1994).

[34] A. Houghton and J. B. Marston, Phys. Rev. B **48**, 7790 (1993).
[35] A. H. Castro Neto and E. Fradkin, Phys. Rev. Lett. **72**, 1393 (1994).
[36] H.-J. Kwon, A. Houghton, and J. B. Marston, Phys. Rev. Lett. **73**, 284 (1994).
[37] S.-S. Lee, P. A. Lee, and T. Senthil, Phys. Rev. Lett. **98**, 067006 (2007).
[38] V. Galitski and Y. B. Kim, Phys. Rev. Lett. **99**, 266403 (2007).
[39] S. Sachdev (private communication).
[40] For example, see J. Polchinski, *String Theory* (Cambridge University Press, Cambridge, England, 1998), Vol. II, Chap. 10.